**PREPARED FOR THE U.S. DEPARTMENT OF ENERGY,
UNDER CONTRACT DE-AC02-76CH03073**

PPPL-3659
UC-70

PPPL-3659

Enhanced Mode Conversion of Thermally Emitted Electron Bernstein Waves (EBW) to Extraordinary Mode

by

B. Jones, P.C. Efthimion, G. Taylor, T. Munsat, J.R. Wilson, J.C. Hosea,
R. Kaita, R. Majeski, R. Maingi, S. Shiraiwa, and J. Spaleta

January 2002

PPPL
PRINCETON PLASMA
PHYSICS LABORATORY

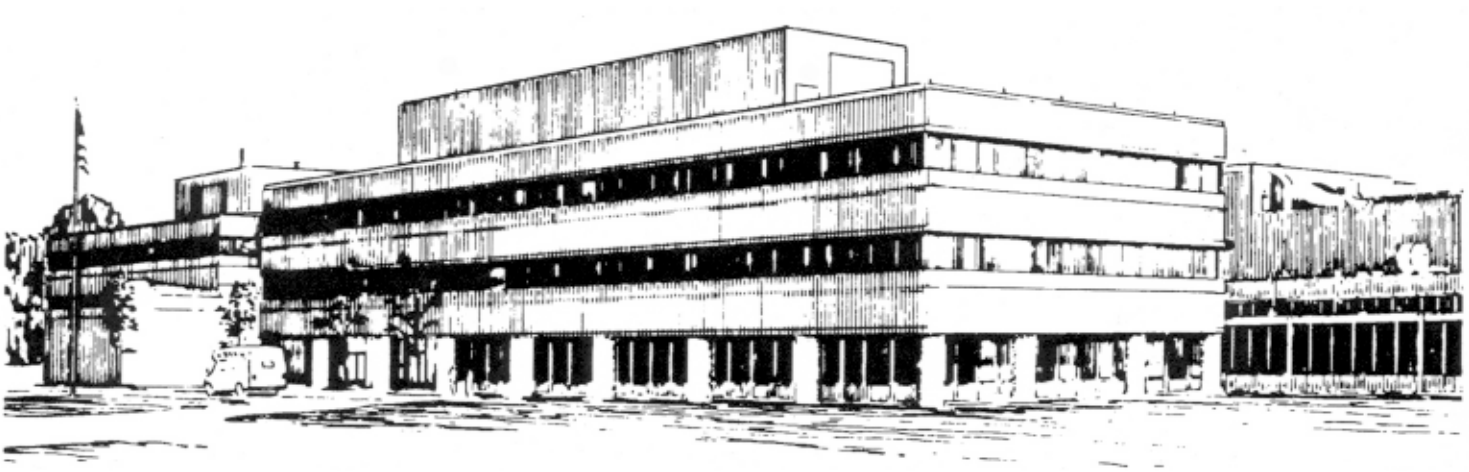

**PRINCETON PLASMA PHYSICS LABORATORY
PRINCETON UNIVERSITY, PRINCETON, NEW JERSEY**

PPPL Reports Disclaimer

This report was prepared as an account of work sponsored by an agency of the United States Government. Neither the United States Government nor any agency thereof, nor any of their employees, makes any warranty, express or implied, or assumes any legal liability or responsibility for the accuracy, completeness, or usefulness of any information, apparatus, product, or process disclosed, or represents that its use would not infringe privately owned rights. Reference herein to any specific commercial product, process, or service by trade name, trademark, manufacturer, or otherwise, does not necessarily constitute or imply its endorsement, recommendation, or favoring by the United States Government or any agency thereof. The views and opinions of authors expressed herein do not necessarily state or reflect those of the United States Government or any agency thereof.

Availability

This report is posted on the U.S. Department of Energy's Princeton Plasma Physics Laboratory Publications and Reports web site in Fiscal Year 2002. The home page for PPPL Reports and Publications is: http://www.pppl.gov/pub_report/

DOE and DOE Contractors can obtain copies of this report from:

U.S. Department of Energy
Office of Scientific and Technical Information
DOE Technical Information Services (DTIS)
P.O. Box 62
Oak Ridge, TN 37831

Telephone: (865) 576-8401

Fax: (865) 576-5728

Email: reports@adonis.osti.gov

This report is available to the general public from:

National Technical Information Service
U.S. Department of Commerce
5285 Port Royal Road
Springfield, VA 22161

Telephone: 1-800-553-6847 or
(703) 605-6000

Fax: (703) 321-8547

Internet: http://www.ntis.gov/ordering.htm

Enhanced Mode Conversion of Thermally Emitted Electron Bernstein Waves (EBW) to Extraordinary Mode

B. Jones,[*] P.C. Efthimion,[*] G. Taylor,[*] T. Munsat,[*] J.R. Wilson,[*] J.C. Hosea,[*]

R. Kaita,[*] R. Majeski,[*] R. Maingi, S. Shiraiwa , J. Spaleta[*]

[*]*Princteon Plasma Physics Laboratory, Princeton University, Princeton, New Jersey 08543*

Oak Ridge National Laboratory, Oak Ridge, Tennessee 37831

Graduate School of Frontier Sciences, University of Tokyo, Tokyo 113-0033, Japan

In the CDX-U spherical torus, ~100% conversion of thermal EBWs to X-mode has been observed by controlling the electron density scale length (L_n) in the conversion region with a local limiter outside the last closed flux surface. The radiation temperature profile agrees with Thomson scattering electron temperature data. Results are consistent with theoretical calculations of conversion efficiency using measured L_n. By reciprocity of the conversion process, prospects for efficient coupling in EBW heating and current drive scenarios are strongly supported.

PACS numbers: 52.55.Fa, 52.35.Hr, 52.35.Mw, 52.70.Gw

In many high-β magnetically confined plasmas, standard electron cyclotron emission (ECE) electron temperature (T_e) profile diagnostics, as well as EC heating and current drive, cannot be employed since the electron plasma frequency is much larger than the electron cyclotron

frequency ($f_{pe}>>f_{ce}$). Fundamental and lower f_{ce} harmonic electromagnetic waves are evanescent in the core of the plasma, and higher harmonics that are accessible do not meet the blackbody emission condition of optical thickness $\tau > 2$. The electron Bernstein wave (EBW) has been proposed as an alternate method for measuring the T_e profile in a high-β plasma. [1,2] Since the EBW is an electrostatic wave it can propagate above the critical density in a magnetized plasma, and is strongly absorbed at the f_{ce} harmonics, with $\tau \approx 300$ in CDX-U. [2,3,4] The EBW can mode-convert to either an O- or X-mode electromagnetic wave at the upper hybrid resonance (UHR) layer. The resulting electromagnetic waves emitted can be measured with an antenna and radiometer as in the standard ECE technique.

Conversion between EBW and O-mode waves via the slow X-mode (B-X-O process) occurs at oblique angles in a narrow range of $n_{//}$ whose optimal value is determined by f_{ce}/f and whose width is generally determined by the electron density scale length (L_n) in the conversion region. [5] This process has been extensively studied in both emission and heating experiments on the W7-AS stellarator, with results in good agreement with theory. [1,6]

EBW conversion to X-mode (B-X process) occurs for $n_{//}\approx 0$ with a mode conversion efficiency (C) sensitively dependent on L_n in the conversion region at the UHR. A 1D slab model results in the analytic theory for $n_{//}=0$ presented in [7]. The full expression for mode conversion efficiency is

$$C = C_{max} \cos^2(\phi/2+\theta) \tag{1}$$

where $\cos^2(\phi/2+\theta)$ is a factor relating to the phasing of the waves in the mode conversion region with $\theta = \arg \Gamma(-i\eta/2)$, and ϕ evaluated in the manner of [8] for the case of the high-field cutoff close to resonance. The maximum mode conversion efficiency (C_{max}) is given by

$$C_{max} = 4e^{-\pi\eta}(1-e^{-\pi\eta}) \tag{2}$$

When the magnetic scale length in the mode conversion region $L_B >> L_n$ as in CDX-U,

$$\eta \approx (2\pi f_{ce} L_n/(c\ \alpha))\ ((1+\alpha^2)^{1/2}-1)^{1/2} \qquad (3)$$

where $\alpha = f_{pe}/f_{ce}$ evaluated at the UHR layer. This conversion is expected to be less sensitively dependent on $n_{//}$, and is the process we have studied in CDX-U. It is also being studied on the MST reversed-field pinch. [9]

Obtaining C~100%, or equivalently radiation temperature $T_{rad} \sim T_e$, requires $L_n \approx 0.5$ cm in CDX-U. Optimizing C is also desirable so that power can be effectively coupled to the plasma for EBW heating and current drive. Studying EBW emission evaluates the same mode conversion physics that affects the inverse processes of heating and current drive [10], so this research tests the viability of proposed X-mode EBW current drive schemes. [11,12]

Further distinguishing emission measurements on CDX-U from those performed on other machines is that in an ST, the mode conversion for lower harmonics typically occurs outside the last closed flux surface (LCFS). L_n can be diagnosed by Langmuir probes and modified by material limiters in this region.

Two independently calibrated, fast frequency scanning, heterodyne radiometers measure fundamental (4-8 GHz) and second harmonic (8-12 GHz) EBW emission every 20 μs. [13] Localization of the EBW emission source to the f_{ce} resonant surfaces has been verified by observing the response of the T_{rad} profile to cooling gas puffs at the plasma edge. [1,14] This justifies a comparison between the measured T_{rad} and Thomson scattering T_e profiles in order to infer a value of C. In previous experiments with an antenna outside a vacuum window on CDX-U, C~10% was observed. [12] Similar observations have been made on NSTX, resulting in good agreement with theoretical C calculated using L_n=1.5 cm, as measured by Thomson scattering.

[15] However, even with the steep edge density profile provided by an NSTX H-mode, a maximum mode conversion efficiency of only 15% was observed.

Rather than relying on the density profile naturally provided by the plasma, it is necessary to create a shorter L_n at the UHR layer outside the LCFS in order to reach C~100%. To meet this goal, an in-vacuum antenna along with a movable local limiter has been installed in CDX-U, shown in Fig. 1. The quad-ridged horn antenna points perpendicular to the LCFS ($n_{//} \approx 0$) on the outboard midplane, oriented with the edge field line pitch so as to measure predominantly X-mode emission with one set of ridges and O-mode with the other. X-mode T_{rad} 2-3 times greater than O-mode T_{rad} is measured, consistent with the lower sensitivity of the O-mode antenna to rays with $n_{//} \neq 0$. The local limiter shortens L_n in the scrape-off layer (SOL) where the B-X mode conversion occurs for f_{ce} and $2\,f_{ce}$, thus optimizing C for ~100% conversion. As the conversion occurs outside the LCFS, the local limiter only modifies the density profile in the SOL immediately in front of the antenna and is not the primary limiter for the plasma.

Also shown in Fig. 1, an array of Langmuir probes adjacent to the antenna measures the density profile in the mode conversion region so that the observed emission can be compared to C calculated using L_n measurements. These 5 mm long cylindrical probes can be swept in voltage to measure T_e or biased negatively to measure ion saturation current (I_{sat}) from which electron density (n_e) can be calculated.

Figure 2 (a) shows the significant steepening of L_n outside the LCFS due to the local limiter. For each point, data were averaged for approximately five shots with similar plasma parameters. I_{sat} was averaged over 0.1 ms during each shot in order to smooth out fluctuations. The profile naturally occurring in the SOL with L_n=3-6 cm (diamonds, dashed line) was measured by scanning the entire assembly, using the furthest inboard tip which is unperturbed by the local

limiter. With the local limiter located near the LCFS and measuring n_e with the probe tips outboard of the limiter (triangles), an average density scale length L_n=0.66±0.07 cm was measured (solid line is a best fit to three points). As will be discussed, this value is consistent with ~100% B-X conversion efficiency.

Using these density profiles, the UHR frequency $f_{UH}=(f_{pe}^2+f_{ce}^2)^{1/2}$ is calculated as a function of major radius in Fig. 2 (b). f_{ce} is calculated using |B| from the equilibrium code JSOLVER constrained to the measured toroidal plasma current (60 kA). [16] Since $B_p<<B_t$ in CDX-U, JSOLVER is expected to provide a reasonable estimate of |B|. An EBW of a given frequency mode-converts when the outgoing wave reaches the radial position at which $f=f_{UH}$. f_{UH} calculated using the natural SOL n_e profile (dashed line) illustrates that in CDX-U, the fundamental and second harmonic EBW mode conversion naturally occurs in the SOL, near the vessel wall at R=70 cm in the case of the 4-8 GHz fundamental emission. With the local limiter present (solid line), the mode conversion for 4-12 GHz occurs in a few-centimeter-wide UHR layer between the limiter and antenna position where L_n is shortened.

The effect of the local limiter on the EBW emission is seen in Fig. 3. With the antenna and local limiter retracted near the vessel wall so that the mode conversion occurs in a region with long L_n, the fundamental emission is observed at a low level (triangles). With the local limiter near the LCFS so that the mode conversion occurs in a region of short L_n, we see the emission increase by an order of magnitude (diamonds, solid line). We also plot the second harmonic T_{rad} (diamonds, dashed line), and note that there is favorable agreement with Thomson scattering T_e data (squares) for both fundamental and second harmonic mode-converted EBW emission with L_n shortened by the local limiter. The hollow temperature profile is typical, and is expected as CDX-U is a short-pulse machine with a plasma duration of ~15 ms. Only a 30% reduction in

second harmonic T_{rad} is seen without the local limiter, likely due to the natural steepening of L_n near the LCFS seen in Fig. 2.

The EBW T_{rad} points were mapped from radiometer frequency to R, with error bars reflecting the frequency resolution of the radiometers shown on selected points. 15% T_{rad} error bars are due to systematic error in the absolute calibration, performed using Dicke-switching of a blackbody source. [17] Data points obscured by cyclotron harmonic overlap or for which the mode conversion region is perturbed by the presence of the antenna are not shown.

The Thomson scattering measurements are taken along a vertical axis (z) at a fixed beam radial position. Plotted in Fig. 3 is the average of two data sets for similar CDX-U discharges measured at the start of the time window in Fig. 4. T_e for each set results from a fit to scattered spectra integrated over 16-48 shots to resolve low photon statistics. Mapping from z to R is performed using canonical CDX-U flux surface shapes. Error bars in R are calculated by perturbing the location of the magnetic axis and the plasma elongation. The mapping of the points to outboard radial positions far from the Thomson laser location is especially sensitive to the shape of the flux surfaces, resulting in larger error bars in R. Points closer to the center of the plasma are not available because the laser beam does not pass through the magnetic axis.

Large fluctuations in the emission signal are observed, which we interpret as being due to variation in L_n resulting from density fluctuations at the local limiter. These fluctuations can be seen in the time evolution of T_{rad} and I_{sat} shown in Fig. 4. The T_{rad} profiles shown in Fig. 3 represent single radiometer sweeps selected at the peak of fluctuating emission within the analysis time window. Vertical arrowed lines show the peak-to-peak fluctuation at 6 GHz and 10 GHz. Note that the fluctuation is greater at 6 GHz, extending down to about 10% of the peak signal, while the 10 GHz fluctuation drops to only about 40% of the maximum T_e.

The n_e profile data from the probes and the EBW emission measurements can test the theory of B-X mode conversion presented in [7]. Fig. 5 (c) shows theoretical mode conversion efficiency C calculated from equation (1) as a function of L_n at both 6 and 10 GHz (fundamental and second harmonic emission frequencies). The average L_n measured behind the local limiter is shown (dashed vertical line), with the shaded region representing the error bars. It is seen that C~100% is theoretically attainable with the short L_n produced by the local limiter, consistent with the comparison between T_{rad} and Thomson T_e profiles. Interpreting the fluctuating emission observed as being due to fluctuations carrying L_n out to near 2 cm (dotted line), we see that the theoretical C drops to 10% for the 6 GHz case and 40% for 10 GHz. This is consistent with the observed fluctuation in the emission signal, as shown in Fig. 3, and with the 0.4 and 3.4 cm worst-case limits on L_n obtained by considering the ranges of fluctuating n_e measured at the probe locations spanning the conversion layer. Note that had we neglected the phase factor and calculated only C_{max} versus L_n (Fig. 5 (a)), we would not have predicted the differing levels of T_{rad} fluctuation observed. It is the frequency dependence in $\cos^2(\phi/2+\theta)$ near L_n~2 cm (Fig. 5 (b)) that leads to this difference in C at 6 and 10 GHz.

Further evidence that fluctuating L_n is playing a role in modifying C, leading to fluctuating emission, is seen by comparing the T_{rad} and probe I_{sat} time evolution. For several probe tip positions, the cross-correlation between these signals was calculated in a time window approximately 1 ms wide. 70% anti-correlation was observed for the probe located 0.6 cm behind the local limiter and emission at 5.5 GHz, which mode-converts near the probe location. The emission peaked when the density behind the limiter dropped, consistent with L_n shortening. Correlation was not seen for probes 2 cm on either side of this location.

100% B-X mode conversion efficiency has been observed in CDX-U by controlling L_n at the UHR layer, allowing direct measurement of the T_e profile from mode-converted EBW emission. The measured T_e profile was similar to that measured by Thomson scattering. C~100% and measured L_n at the UHR are consistent with the theory of [7]. The $\cos^2(\phi/2+\theta)$ phase factor in this theory has been found to be important, and explains the frequency dependence of the observed T_{rad} fluctuations. Since the mode conversion occurs in the SOL for an ST, L_n can be controlled and optimized with a local limiter that does not perturb the plasma. Similarly, reciprocity of the mode conversion process is a strong justification for using a local limiter with an X-mode electromagnetic heating or current drive antenna to achieve efficient coupling to the EBW branch.

The authors would like to thank the CDX-U technical staff and T. Kramer for their contributions. This work was supported by DOE Contract No. DE-AC02-76-CHO-3073 as part of the Innovations in Magnetic Fusion Energy Diagnostic Systems program.

[1] H. P. Laqua *et al.*, Phys. Rev. Lett. **81**, 2060 (1998).

[2] P. C. Efthimion *et al.*, Rev. Sci. Instrum. **70**, 1018 (1999).

[3] J. Hosea, V. Arunasalam, and R. Cano, Phys. Rev. Lett. **39**, 408 (1977).

[4] T. Jones, Ph.D. Thesis, Princeton U. (1995).

[5] J. Preinhaelter and V. Kopecky, J. Plasma Phys. **10**, 1 (1973).

[6] H. P. Laqua *et al.*, Phys. Rev. Lett. **78**, 18 (1997).

[7] A. K. Ram and S. D. Schultz, Phys. Plasmas **7**, 4084 (2000).

[8] A. K. Ram *et al.*, Phys. Plasmas **3**, 1976 (1996).

[9] P. K. Chattopadhyay *et al.*, AIP Conference Proceedings **595**, 346 (2001).

[10] A. K. Ram, A. Bers, and C. N. Lashmore-Davies, Phys. Plasmas **9**, 409 (2002).

[11] C. B. Forest *et al.*, Phys. Plasmas **7**, 1352 (2000).

[12] G. Taylor *et al.*, AIP Conference Proceedings **595**, 282 (2001).

[13] G. Taylor *et al.*, Rev. Sci. Instrum. **72**, 285 (2001).

[14] T. Munsat *et al.*, Phys. Plasmas **9**, 480 (2002).

[15] G. Taylor *et al.*, Phys. Plasmas **9**, 167 (2002).

[16] J. Delucia *et al.*, J. Comput. Phys. **37**, 183 (1980).

[17] R. H. Dicke, Rev. Sci. Instrum. **17**, 268 (1946).

FIG. 1. The CDX-U EBW diagnostic combines a quad-ridged horn antenna to measure emission, a movable local limiter (half shown) to modify L_n in front of the antenna to optimize mode conversion, and a Langmuir probe array to measure L_n.

FIG. 2. (a) The L_n=3-6 cm electron density profile naturally occurring in the SOL (diamonds, dashed line) and the L_n=0.66–0.07 cm profile created by the local limiter (triangles, solid line). (b) The corresponding UHR frequency profiles, determining the mode conversion location for a wave of frequency $f = f_{UH}$. The local limiter creates a narrow mode conversion layer in front of the antenna for the fundamental and second harmonic EBW frequency ranges (shown shaded).

FIG. 3. The radiation temperature without the local limiter (triangles). With the local limiter, the peak fundamental emission (diamonds, solid line) and second harmonic emission (diamonds, dashed line) together map out the T_e profile and are consistent with T_e measured by Thomson scattering (squares). The emission fluctuation levels at 6 and 10 GHz are indicated by vertical arrowed lines.

FIG. 4. Time evolution of a typical CDX-U discharge. (a) Toroidal plasma current, (b) line-averaged density (R=35 cm), (c) ion saturation current from Langmuir probes showing edge n_e fluctuation (local limiter at R=56.6 cm, data from two separate shots), and (d) EBW T_{rad} at 10 GHz, showing multiple peaks resulting from gas puff modulation and fluctuation resulting from changing L_n. Analysis was performed in the shaded time window.

FIG. 5. (a) The maximum mode conversion efficiency C_{max} for 6 GHz (solid) and 10 GHz (dashed) emission as a function of L_n just outside the CDX-U LCFS, (b) the $\cos^2(\phi/2+\theta)$ phase factor, and (c) the theoretical mode conversion efficiency $C=C_{max}\cos^2(\phi/2+\theta)$.

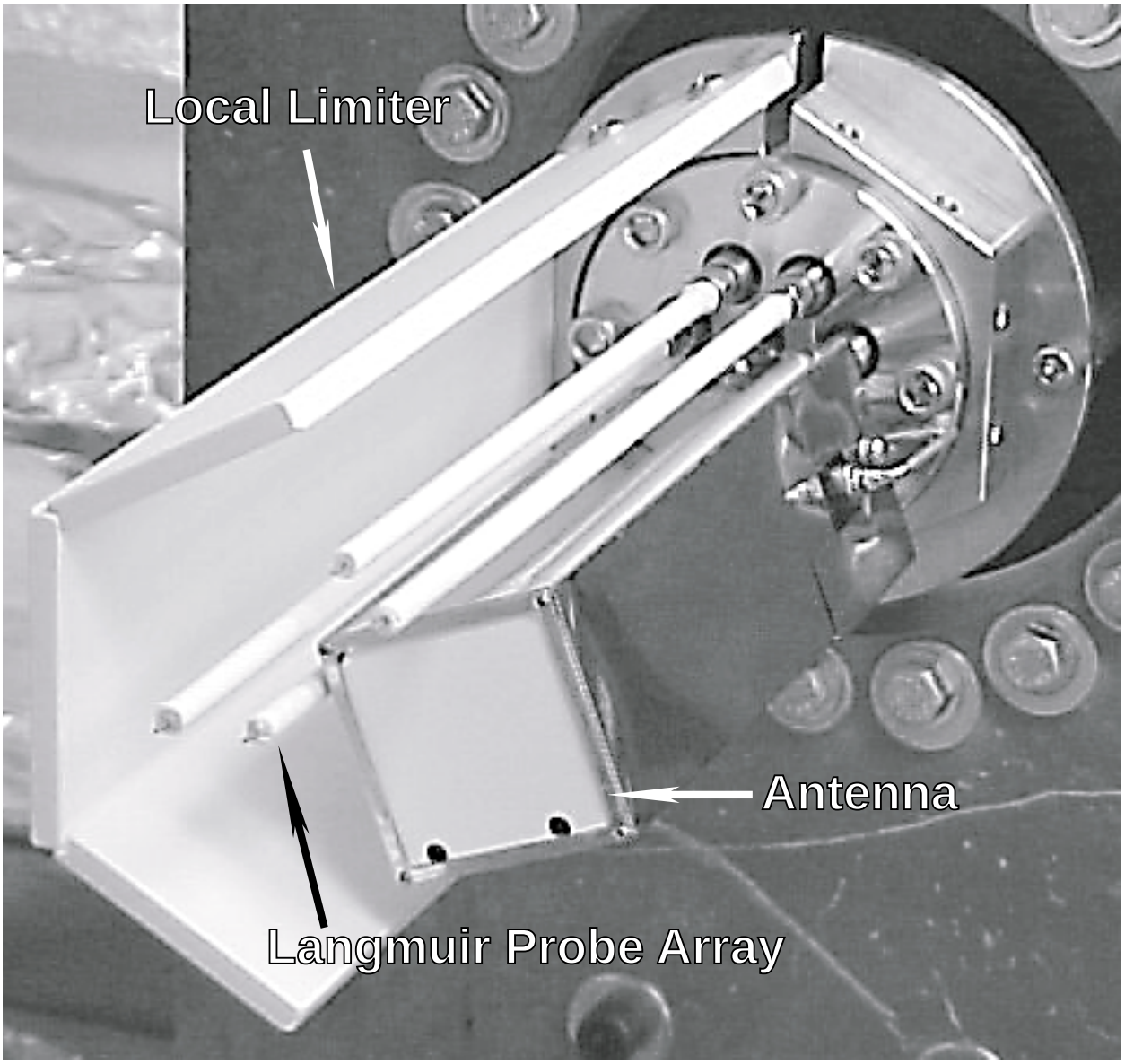

FIGURE 1, B. Jones, Phys. Rev. Lett.

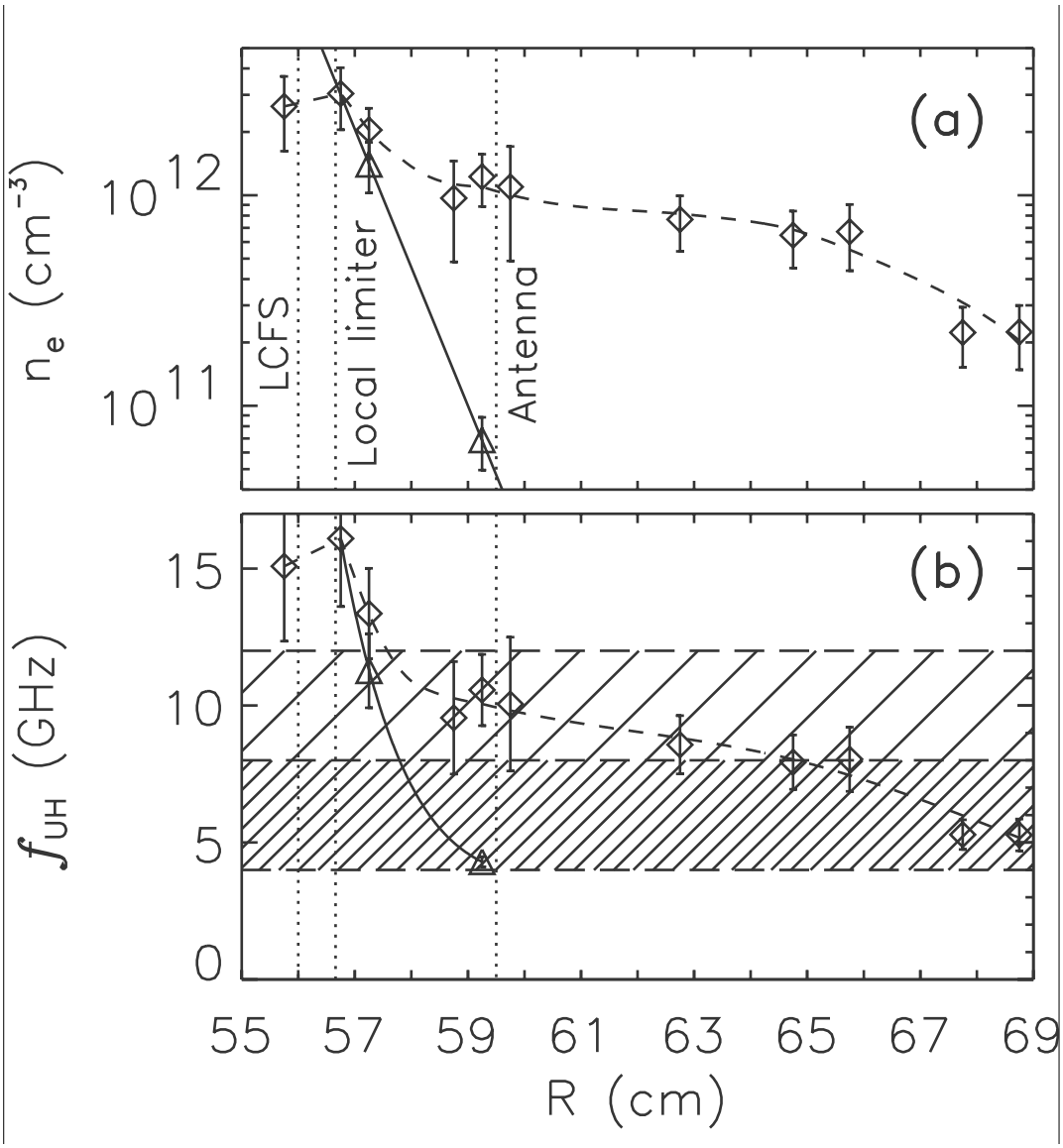

FIGURE 2, B. Jones, Phys. Rev. Lett.

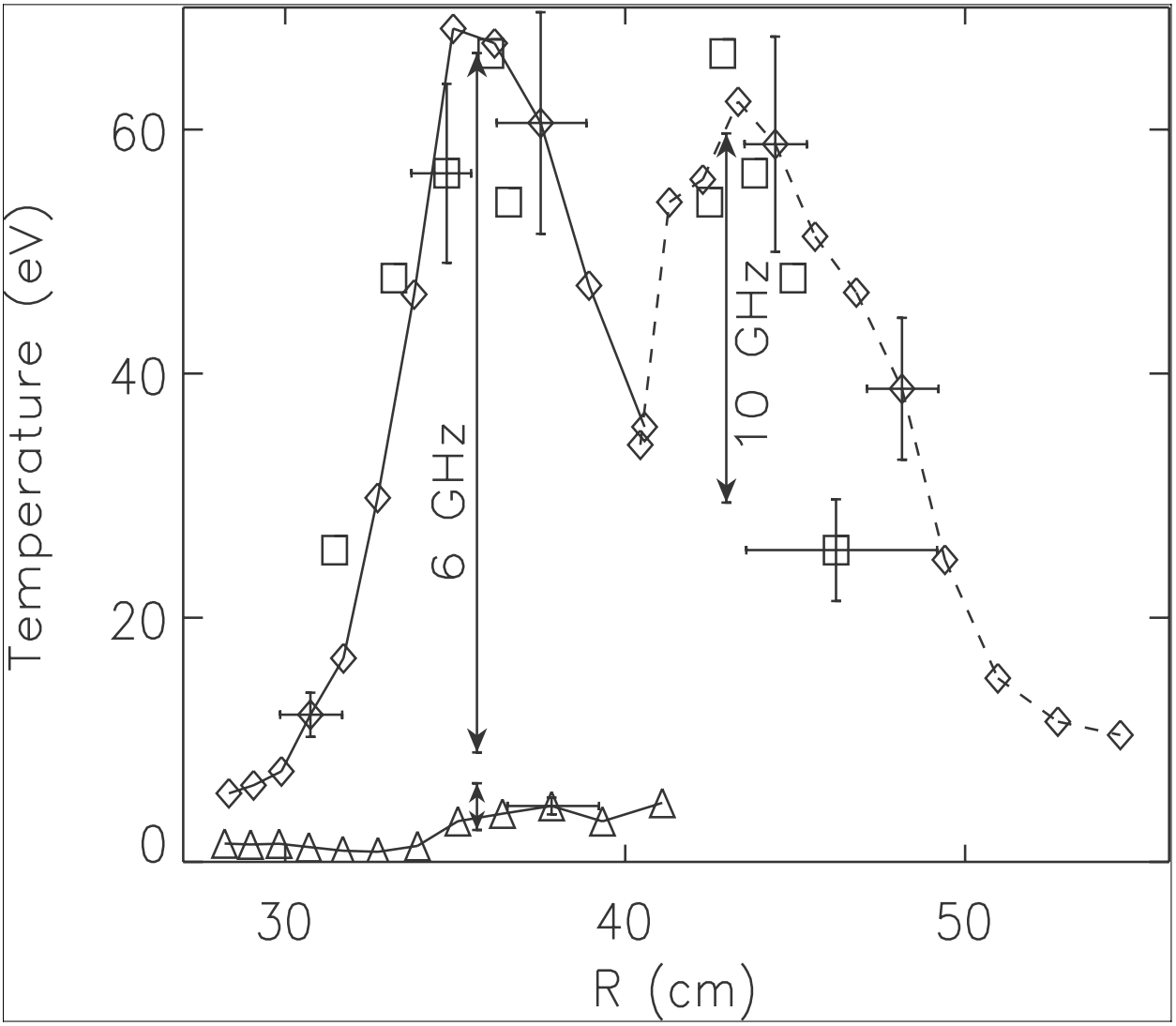

FIGURE 3, B. Jones, Phys. Rev. Lett.

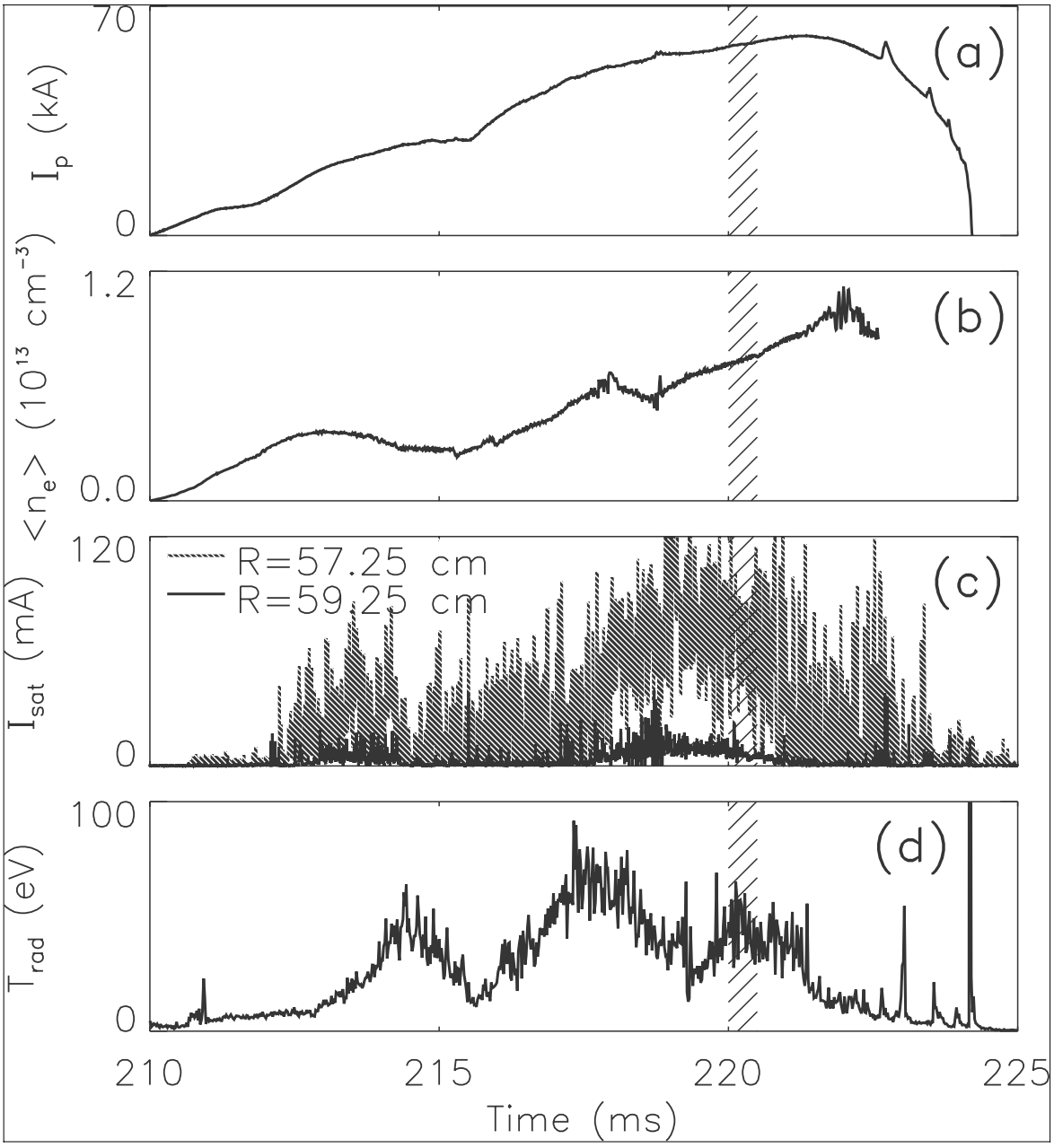

FIGURE 4, B. Jones, Phys. Rev. Lett.

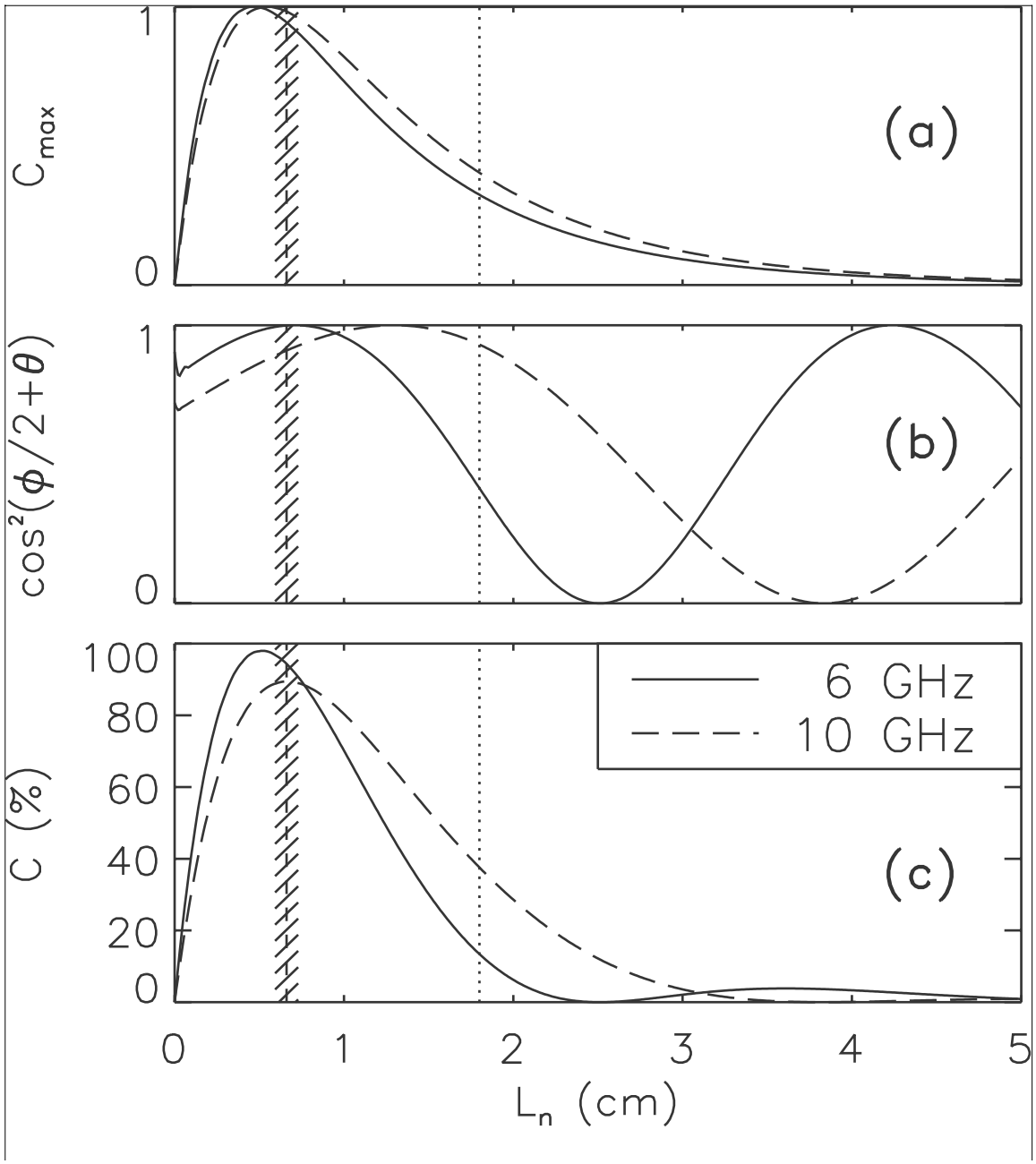

FIGURE 5, B. Jones, Phys. Rev. Lett.

External Distribution

Plasma Research Laboratory, Australian National University, Australia
Professor I.R. Jones, Flinders University, Australia
Professor João Canalle, Instituto de Fisica DEQ/IF - UERJ, Brazil
Mr. Gerson O. Ludwig, Instituto Nacional de Pesquisas, Brazil
Dr. P.H. Sakanaka, Instituto Fisica, Brazil
The Librarian, Culham Laboratory, England
Library, R61, Rutherford Appleton Laboratory, England
Mrs. S.A. Hutchinson, JET Library, England
Professor M.N. Bussac, Ecole Polytechnique, France
Librarian, Max-Planck-Institut für Plasmaphysik, Germany
Jolan Moldvai, Reports Library, MTA KFKI-ATKI, Hungary
Dr. P. Kaw, Institute for Plasma Research, India
Ms. P.J. Pathak, Librarian, Insitute for Plasma Research, India
Ms. Clelia De Palo, Associazione EURATOM-ENEA, Italy
Dr. G. Grosso, Instituto di Fisica del Plasma, Italy
Librarian, Naka Fusion Research Establishment, JAERI, Japan
Library, Plasma Physics Laboratory, Kyoto University, Japan
Research Information Center, National Institute for Fusion Science, Japan
Dr. O. Mitarai, Kyushu Tokai University, Japan
Library, Academia Sinica, Institute of Plasma Physics, People's Republic of China
Shih-Tung Tsai, Institute of Physics, Chinese Academy of Sciences, People's Republic of China
Dr. S. Mirnov, TRINITI, Troitsk, Russian Federation, Russia
Dr. V.S. Strelkov, Kurchatov Institute, Russian Federation, Russia
Professor Peter Lukac, Katedra Fyziky Plazmy MFF UK, Mlynska dolina F-2, Komenskeho Univerzita, SK-842 15 Bratislava, Slovakia
Dr. G.S. Lee, Korea Basic Science Institute, South Korea
Mr. Dennis Bruggink, Fusion Library, University of Wisconsin, USA
Institute for Plasma Research, University of Maryland, USA
Librarian, Fusion Energy Division, Oak Ridge National Laboratory, USA
Librarian, Institute of Fusion Studies, University of Texas, USA
Librarian, Magnetic Fusion Program, Lawrence Livermore National Laboratory, USA
Library, General Atomics, USA
Plasma Physics Group, Fusion Energy Research Program, University of California at San Diego, USA
Plasma Physics Library, Columbia University, USA
Alkesh Punjabi, Center for Fusion Research and Training, Hampton University, USA
Dr. W.M. Stacey, Fusion Research Center, Georgia Institute of Technology, USA
Dr. John Willis, U.S. Department of Energy, Office of Fusion Energy Sciences, USA
Mr. Paul H. Wright, Indianapolis, Indiana, USA

The Princeton Plasma Physics Laboratory is operated
by Princeton University under contract
with the U.S. Department of Energy.

Information Services
Princeton Plasma Physics Laboratory
P.O. Box 451
Princeton, NJ 08543

Phone: 609-243-2750
Fax: 609-243-2751
e-mail: pppl_info@pppl.gov
Internet Address: http://www.pppl.gov